© Universiti Tun Hussein Onn Malaysia Publisher's Office

IJIE

Journal homepage: http://penerbit.uthm.edu.my/ojs/index.php/ijie
ISSN : 2229-838X e-ISSN : 2600-7916

The International Journal of Integrated Engineering

Improved Mechanical Properties and In-Vitro Degradation of Chitosan-Pristine Graphene Nanocomposites

Farid Wajdi[1,2], Indraswari Kusumaningtyas[1], Andi R. Wijaya[1], Alva E. Tontowi[1*]

[1]Department of Mechanical and Industrial Engineering,
Universitas Gadjah Mada, Jl. Grafika2, Yogyakarta, 55281, INDONESIA

[2]Department of Industrial Engineering,
Universitas Serang Raya, Jl. Raya Serang-Cilegon KM 5, Serang, 42116, INDONESIA

*Corresponding Author

DOI: https://doi.org/10.30880/ijie.2021.13.01.020
Received 20 November 2019; Accepted 3 February 2020; Available online 30 January 2021

Abstract: Studies over the use of pristine graphene as reinforcement for biopolymers are rarely found. In this study, we prepared biodegradable chitosan and pristine graphene nanocomposites films with a small amount of glycerol to enhance the bonding. The aim was to study the mechanical improvement and degradation rates of the nanocomposites material. Characterizations of the nanocomposites consist of a Fourier Transform Infrared (FTIR), Scanning Electron Microscopy (SEM), tensile and degradation testing. The results showed that 1% wt of glycerol improved graphene dispersion throughout the chitosan matrix due to the hydrogen bonding and electrostatic interactions between chitosan and graphene grapheme. To some extent, the addition of 0.2 to 0.4% wt of pristine graphene improved the stiffness and tensile strength of chitosan that is emphasized by the glycerol. However, glycerol concentration should be increasing at an increased level of graphene in the chitosan matrix to prevent graphene agglomeration. In 0.6% wt of graphene contained chitosan films,

Keywords: Pristine graphene, chitosan, nanocomposites, mechanical properties, degradation

1. Introduction

Chitosan is an abundant natural biopolymer, sourced from the shellfish waste such as crustaceans and crabs. Its structure is derived from chitin processed by the chemical deacetylation. Due to its nontoxicity, biodegradability, biocompatibility, bioactivity, and antimicrobial nature, chitosan is very useful for many applications, including biomedical, pharmaceutical, chemical, agriculture, and environmental fields [1], [2].

Chitosan is brittle and water sensitive because of its hydrophilic nature. Its mechanical properties are comparable to commercial polymers based on cellulose [3]. For specific applications where mechanical strength is needed, chitosan requires property enhancements of its mechanical weaknesses [4]. Forming the composites materials and blending with both synthetic and natural polymers are methods to modify chitosan properties. Different kinds of nanofillers have been used such as zinc oxides, magnesium oxides, bamboo, montmorillonite [5]–[7]. A number of studies have prepared chitosan with poly(l-lactic acid), polycaprolactone, and starch [7]–[13].

In the biomedical engineering field, studies over chitosan as scaffold material have been done. Lauto et al. [14] have prepared chitosan-based scaffolds for the treatment of obstruction in urology and gastroenterology. They have inhibited quick degradation rates of chitosan by immersing the chitosan film into NaOH. Chitosan blending with epoxy [15] and genipin [16] have been studied to prepare infrarenal aorta stent with the self-expandable mechanism. The use

*Corresponding author: alvaedytontowi@ugm.ac.id

of genipin has improved the flexibility and biocompatibility of chitosan. In cardiovascular therapy, chitosan has been used as the stent cover membrane in aneurysm treatment to reduce embolic complication [17].

In a recent development, researchers have applied graphene nanofillers in various materials, including chitosan nanocomposites [18]–[23]. Based on the studies over graphene-coated or graphene-built scaffolds, graphene will find its applications for development of the future endovascular materials [24]. It has certain advantages over existing metallic scaffolds, such as lower thrombogenicity. Therefore, graphene-based scaffolds could improve long-term patency and less allergic reactions endovascular scaffolds. Graphene oxide is commonly studied in graphene-based chitosan nanocomposites. Graphene oxide is a graphene derivate with oxygenated functionalities. Due to its higher compatibility with the functional groups of biopolymers, it forms better bonding with the polymer matrix. However, obtaining graphene oxide is a much more complicated process and expensive. Pristine graphene is another derivate of graphene materials that have no oxygen functionalities. Its synthesis process is much simpler and without the use of toxic reagents. The mechanical exfoliation method is one of the approaches to obtain graphene for lab scale.

This article reports the preparation of chitosan-pristine graphene nanocomposites using the solvent casting method. Pristine graphene nanofillers were synthesized from natural graphite powders by mechanical exfoliation method in the liquid-phase [25]–[27]. The blending of chitosan-pristine graphene nanocomposites enhanced by a small amount of glycerol (1% w/v). Characterization of various performance parameters includes Fourier Transfer infrared (FTIR), mechanical testing, Scanning Electron Microscope (SEM), and in-vitro degradation.

2. Materials and Methods

2.1 Materials

Commercial food-grade chitosan (>95% purity, 800 kDa) was purchased from Chimultiguna (Cirebon, Indonesia). Natural graphite powder (60 mesh, >95% carbon) was provided by the Product Design & Development Lab (UGM, Indonesia). Other reagents were provided by the LPPT Lab (UGM, Indonesia). All materials were used as received.

2.2 Preparation of Graphene

Two grams of graphite were irradiated by a microwave oven for 3 minutes to expand the distance between the graphite layers. Then the graphite was put into 300 ml aquadest containing 0.5 g Sodium Dodecyl Sulphonate (SDS) surfactant. We used a Philips HR2071 blender and a Sonicator Branson 3800 (40 kHz) water bath to exfoliate the suspension for 60 minutes each. The graphene platelets were obtained by centrifugation for 30 minutes at 7500 rpm and washed twice with aquadest. The graphene platelets were dried at ambient temperature and collected for the following use.

2.3 Preparation of Chitosan Film

Four grams of chitosan powders were dissolved in 200 ml 1% acetic acid solution gradually to prevent clotting upon stirring. It formed a homogenous solution after 4 hours of stirring. The chitosan solution was then poured into a melamine tray and left at room temperature to evaporate water and acetic acid for five days. Finally, the as-prepared film was dried under an incubator at 40^0C for two days and coded as Cs.

2.4 Preparation of Chitosan-Glycerol-Graphene Nanocomposites Films

A similar procedure was done to produce chitosan-glycerol-graphene films. Chitosan and glycerol were mixed in 200 ml 1% acetic acid solution by stirring for 4 hours. Different loadings of pristine graphene were prepared by dispersing in 40 ml of 1% acetic acid by stirring and sonication for 30 minutes each. We blended the graphene suspension and chitosan-glycerol 1% (w/v) solution while stirring. We obtained a homogeneous suspension of chitosan-glycerol-graphene after 2 hours of stirring. The suspension was dried as same as the fabrication of chitosan film. The produced thin chitosan-glycerol-graphene nanocomposites films were used for the characterizations. The procedure was repeated for making all samples and coded as CsGlyG 00, CsGlyG 02, CsGlyG 04, and CsGlyG 06 respectively.

2.5 Preparation of Simulated Body Fluid (SBF)

Simulated Body Fluid (SBF)-Tris is the soaking medium for the degradation testing, developed by Tas [28]. It is a modified recipe of the Kokubo SBF [29]. The composition of the SBF solution is an imitation of the human blood plasma. The 1000 ml SBF-Tris is composed of 960 ml deionized water and the following compounds: 6.5456 mg NaCl, 2.2682 g $NaHCO_3$, 0.373 g KCl, 0.1419 g $Na_2HPO_4.2H_2O$, 0.3049 g $MgCl_2x6H_2O$, 9 ml 1M HCl, 0.3675 g $CaCl_2x2H_2O$, 0.071 g Na2SO4, 6.057 g Tris $(CH_2OH)_3$ CNH_2. All compounds were dissolved one by one using a magnetic stirrer. SBF-Tris with the 7.4 pH was achieved by dripping 1M HCL gradually while maintaining the temperature at 37°C. The solution was put into a tightly capped bottle and stored in a 4°C refrigerator for use in the degradation testing.

2.6 Characterizations

Fourier Transform Infra-Red (FTIR) analyses were performed to study the interaction between chitosan-pristine graphene film matrices at the microscopic level. IR spectra were recorded using a Shimadzu IRPrestige spectrophotometer with potassium bromide (KBr) as the mulling agent.

The mechanical properties of the chitosan-pristine graphene nanocomposite were tested according to the ASTM-D882-02 standard. The gauge dimension of the testing specimens was 100 x 25 mm and ca. 0.21 mm thickness. Uniaxial tensile tests were done in a Hung Ta Material Testing Machine HT-2402 (Taiwan) equipped with a 5 KN load capacity. The crosshead speed was 10 mm/min. The tensile parameter values were obtained from the nominal stress-strain curves and determined the tensile strength, Young's modulus, yield strength, and elongation at break. All specimens were tested at room temperature (23ºC, 50 RH) by quintuplicate. Average values and their deviations were reported.

The fracture surface of the testing specimen was observed by a Scanning Electronic Microscopy (SEM) JEOL JSM-6510. The sample was mounted on metal grids, covered with a thin layer of platinum, and was conditioned in an ion-sputtering device JEOL JEC-3000FC Auto Fine Coater, as a specimen preparation apparatus for an SEM. The micrographs were taken between 500 and 10000X enlargements.

In-Vitro Degradation testing was performed by cutting the 10 x 10 mm film specimens. The specimens were weighted and put in the glass tubes filled with SBF-Tris solution (pH 7.4, 37 ◦C). We placed the samples in an incubator to keep the temperature constant. The specimens were investigated in the five intervals periods: 7, 14, 21, 28, and 35 days. The samples were removed from the tubes at the time intervals and wiped gently using soft filter papers and weighted for the swelling ratio by using analytical balance Ohaus CP214. Afterward, the samples were dried in the incubator at 37ºC for 24 hours. The dried samples were weighed again to determine the weight loss (%) or degradation of the films. The swelling and degradation ratios were calculated using the (1] and (2], respectively.

$$S = \frac{W_s - W_i}{W_i} 100\% \quad (1)$$

$$D = \frac{W_i - W_d}{W_i} 100\% \quad (2)$$

The swelling ratio (S) is defined by the increase of the swollen weighed specimen after immersing (W_s-W_i) and divided by its initial weight (W_i). For degradation ratio (D), it is defined by the decrease of the specimen weight after drying (W_i-W_d) and divided by the initial weight of film before immersing (W_i). All experiments have been performed in triplicate.

2.7 Statistics

The statistical significance of the process parameters was determined by using the one-way analysis of variance (ANOVA) procedure. Subsequently, the Tukey's post hoc test was performed for means of groups in homogeneous subsets. The statistical analyses were set at a 95% confidence interval ($\alpha = 0.05$).

3. Results and Discussions

3.1 FTIR

FTIR spectra were obtained for five specimens and showed in **Error! Reference source not found.** and . The presence of glycerol affected the stretching at the O-H peak due to O-H integration from chitosan and glycerol. Chitosan-pristine graphene nanocomposites were functionalized satisfactorily in the chitosan matrices due to glycerol presence. As presented in the graph, CsGlyG 0.2% shows the peak at O-H 3247 cm^{-1}, presenting graphene is functionalized by chitosan and glycerol. Then the O-H wavenumber shifts to 3269 cm^{-1} stacked with O-H groups from chitosan and glycerol into graphene. It is also confirmed by the shift in the vibration wave strain C-H at 2924 cm^{-1} (graphene), shifting to 2921 cm^{-1}. Wavenumber C=C aromatic at 1627 cm^{-1} (graphene) shifts to 1547 cm^{-1}. The shift and accumulation of the wavenumbers prove that chitosan and glycerol were functionalized with graphene. Since graphene was synthesized using an SDS surfactant, which is a rich oxygenated substance, structure C-O stretching at 1026 cm^{-1} was observed [30].

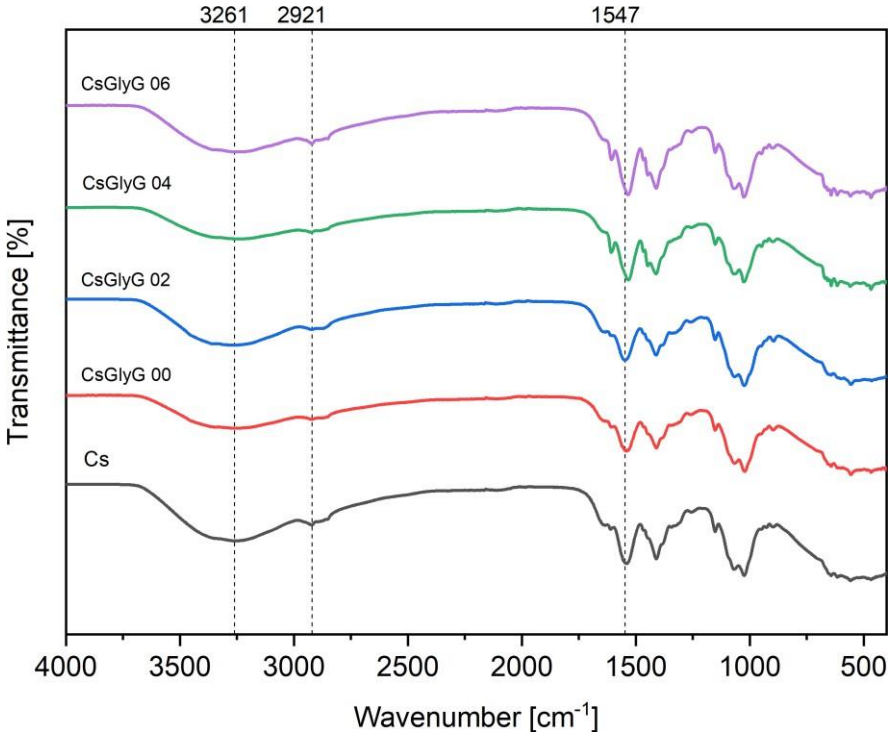

Fig. 1 - FTIR spectra of chitosan-glycerol-graphene nanocomposites

Table 1 - Chitosan/graphene with glycerol

Components	Cs	CsGlyG 0.0	CsGlyG 0.2	CsGlyG 0.4	CsGlyG 0.6
OH	3261.12	3247.30	3269.16	3254.83	3248.82
CH	2921.21	2921.67	2921.93	2922.68	2920.88
		1408.56	1410.69	1410.76	1410.08
C=C	1538	1534.88	1547.07	1531.87	1532.01
C-O	1068.74	1066.97	1023.28	1069.79	1069.43
	1024.27	1021.49	1066.72	1026.69	1025.72

3.2 Mechanical Properties

The **Error! Reference source not found.**

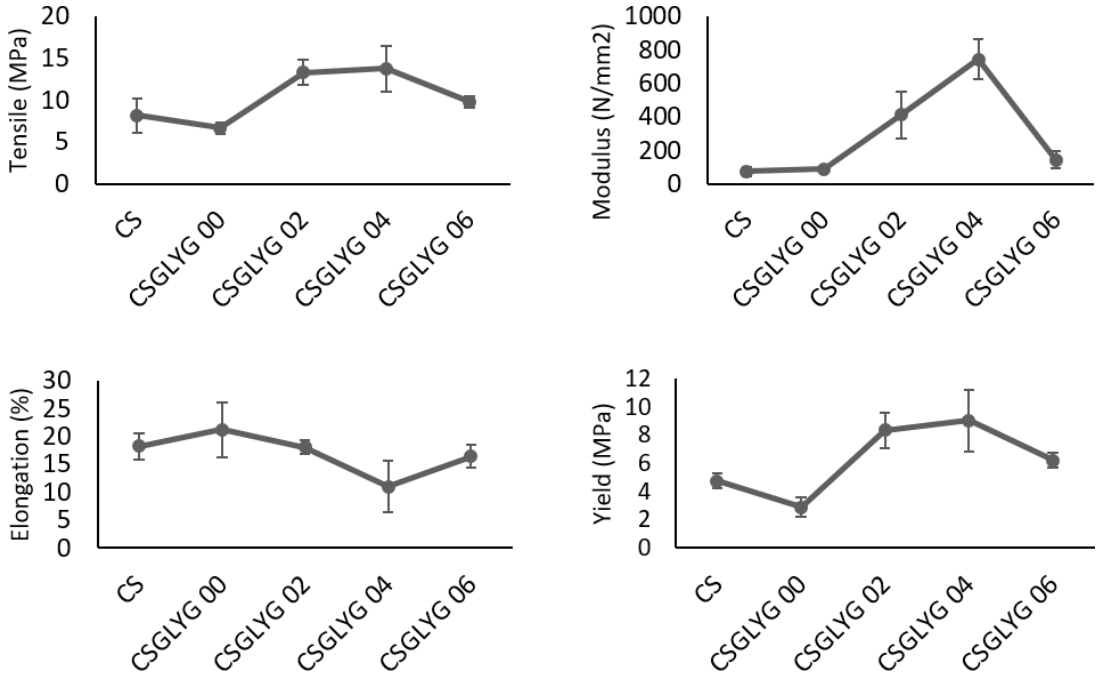

Fig. 2baseline chitosan (Cs) exhibited a tensile strength of 8.18 MPa and Young's modulus of 72.56 MPa. The addition of glycerol has reduced the hydrogen bonds. In other words, the intermolecular forces of the polysaccharide chain of chitosan become smoother and more flexible. As observed in Fig. 2, the modulus and elongation at break of CsGlyG 00 increased by 88.18±10.418 and 19.20±4.764, respectively ($P \leq 0.05$). While the tensile strength decreased at 6.65±0.661 MPa ($P \leq 0.05$).

The addition of graphene in different loadings showed different mechanical behaviors of the chitosan films. The tensile strength of the specimens with graphene concentration up to 0.4% showed a significant increase of about 1.7 folds (13.79±2.73 MPa) from the baseline Cs ($P \leq 0.05$). The increase in the mechanical properties reveals a functional interaction between graphene and the chitosan matrices. However, at the higher graphene concentration represented by CsGlyG 06, its tensile strength decreased by 9.79±0.72 MPa. The declining tendency at higher concentration of graphene may be caused by poor dispersion of the graphene in the chitosan matrix. Higher loading of graphene nanocomposites tends to agglomerate in a polymer matrix, which results in lower fracture strength of the nanocomposites [31], [32]. The increase of glycerol concentration may lead to stabilizing the dispersion of an increased quantity of graphene. Compared to all the results of this mechanical test, CsGlyG 02 presented less change in mechanical properties. While CsGlyG 04 showed increased tensile strength, Young's modulus, and yield strength and decreased elongation at break from the baseline.

Table 2 - Mechanical properties of chitosan-pristine graphene nanocomposites

Sample	Tensile Strength (MPa)	Young's Modulus (N.mm)	Yield Strength (MPa)	Elongation at break (%)
Cs	8.18±2.031	72.56±27.717	4.76±0.698	18.20±4.970
CsGlyG 00	6.65±0.661	88.18±10.418	2.89±0.522	19.20±4.764
CsGlyG 02	8.18±2.030	411.72±139.950	4.76±0.700	18.20±4.970
CsGlyG 04	13.79±2.730	742.79±119.070	9.04±2.210	11.00±4.580
CsGlyG 06	9.79±0.720	143.86±49.860	6.21±0.550	16.40±2.070

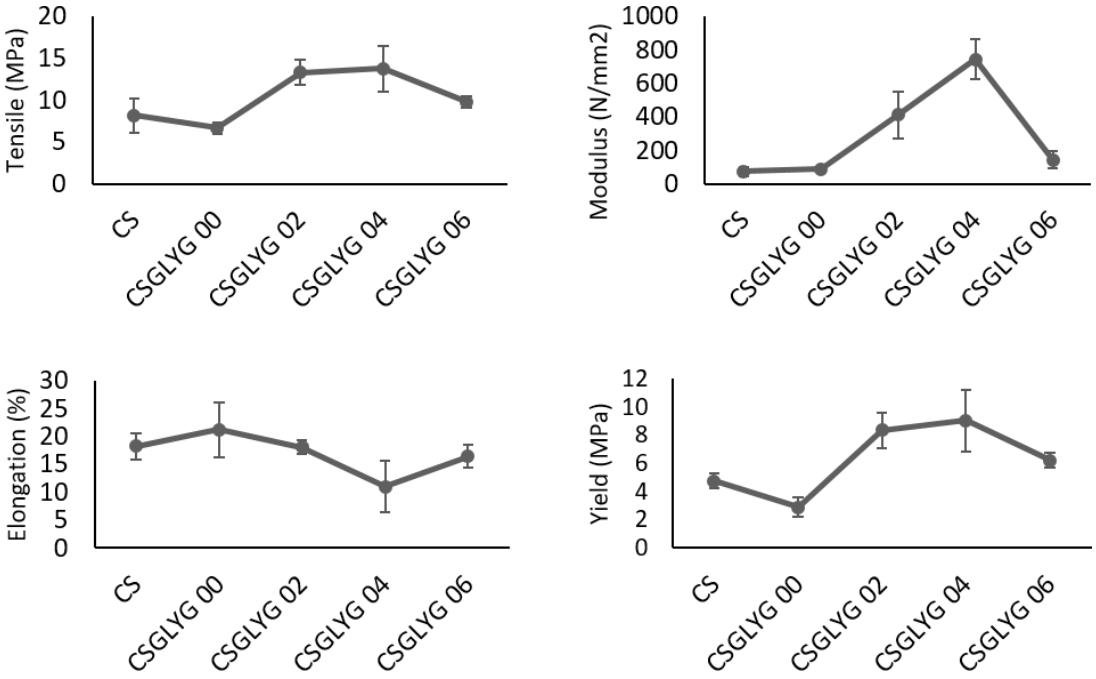

Fig. 2 - Mechanical properties of chitosan-pristine graphene nanocomposites

3.3 SEM

The micrographs of fractography CsGlyG 0.6 nanocomposite at different magnifications are shown in **Error! Not a valid bookmark self-reference**. The cross-section image shows a relatively rough fracture surface of the graphene sheet membranes [21], [33]. The images exhibit clear visibility of dispersed graphene in the chitosan matrix which is rarely visible in low weight concentration [34]. The rough fracture surface is attributed to the interfacial adhesion and compatibility between polymer matrix and graphene nanosheets. However, it seems that graphene aggregates are observed in the SEM images. We observed several small holes here as well. The air bubbles may be trapped during the fabrication process.

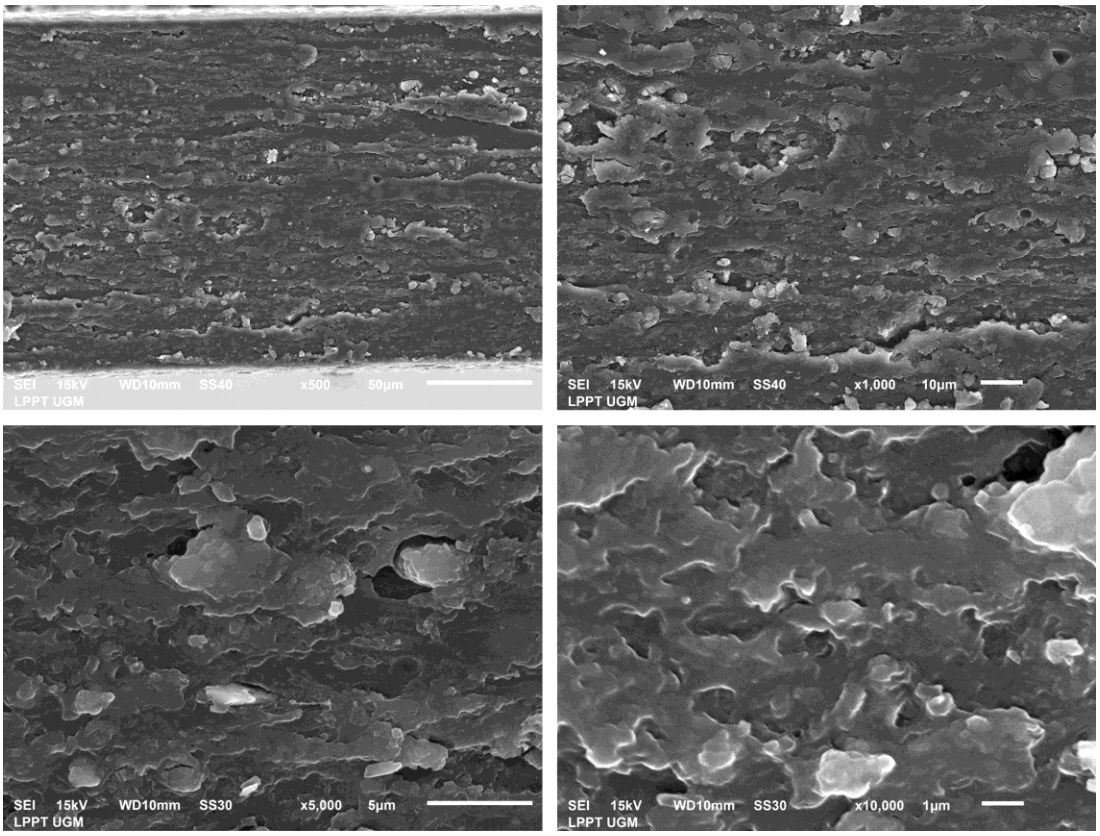

Fig. 3 - SEM images of fracture surface CsGlyG 06 at various magnifications

3.4 Degradation

After incubation of 35 days in the SBF-Tris solution, no significant swelling observed in the samples ($P \geq 0.05$). The swelling ratios (Fig. 4) of the chitosan-graphene nanocomposites increased sharply until the 14th day in the range of 40-60%. After that, it started to stabilize at around 60-70%. All of the films remain almost intact in the SBF medium up to 28 days. However, the chitosan films (Cs) became very fragile after 35 days. The longer interactions of the films and the soaking medium, the lower water up-takes and swellings. The equilibrium swelling % was achieved at about 50-60%.

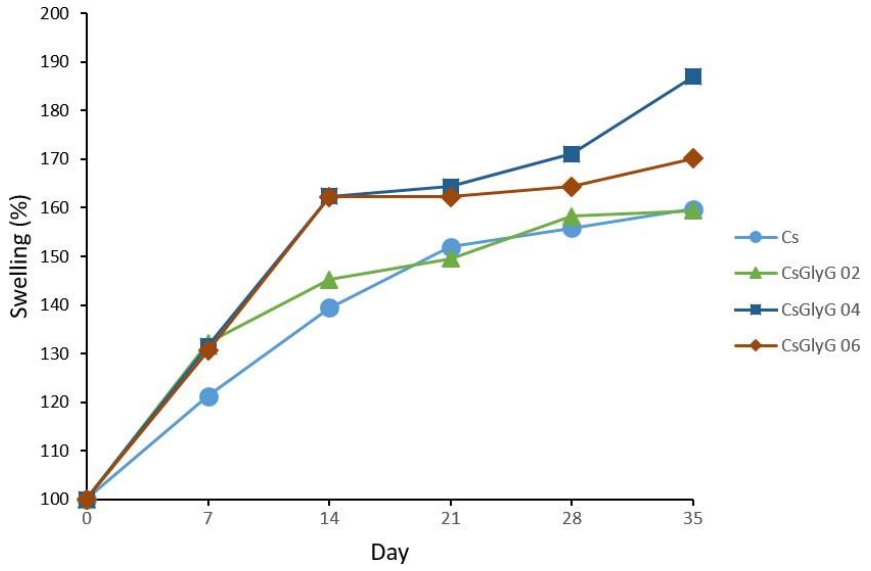

Fig. 4 - Swelling rates

In the degradation observation, there is a difference between the degradation rates before and after seven days of immersion intervals. The weight loss of the specimens decreased quickly up to 45% and started to stabilize afterward. **Fig. 5Fig. 5 - Degradation rates**shows that the degradation rate of chitosan was most accelerated compared to the others. The decrease in its semi-crystalline structure increases the degradation rate [35]. The degradation rate of the different ratios of chitosan-graphene nanocomposites showed quickly hydrolyzed with the existence of water [36]. In this study, there is no significant difference in the degradation rates of the prepared samples ($P \geq 0.05$).

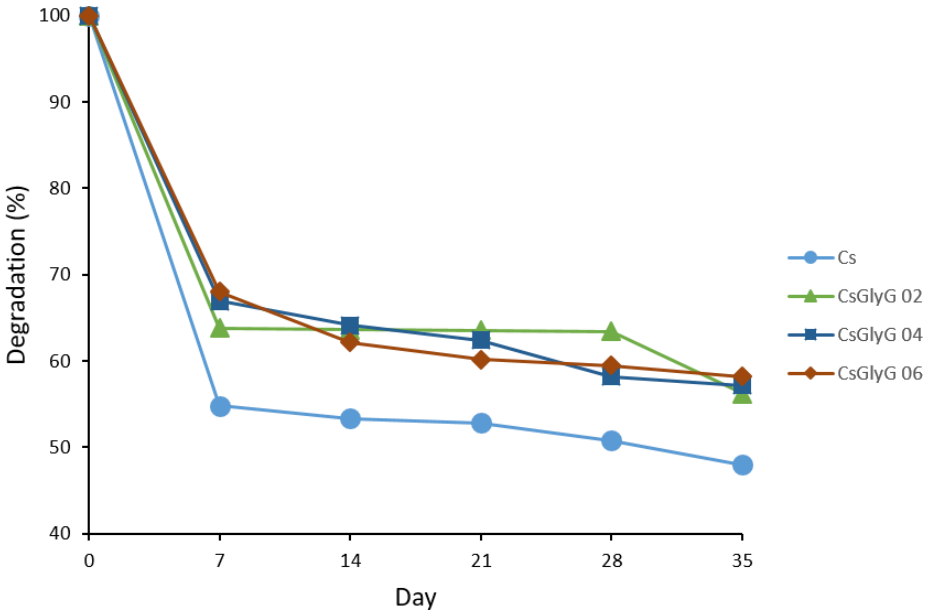

Fig. 5 - Degradation rates

4. Conclusions

Chitosan and pristine graphene nanocomposites were successfully prepared by a solvent casting method. Small loading of glycerol improved the functionalization of graphene in the chitosan matrix. IR spectroscopy of chitosan-pristine graphene indicated the existence of hydrogen bonding interactions between chitosan and graphene. Small loading of glycerol plasticizer (1% wt) has improved the mechanical properties of the chitosan-pristine graphene up to 0.4% wt due to the homogeneous dispersion of pristine graphene in the chitosan matrix and strong interfacial interactions between them. The CsGlyG 04 sample film is the optimum concentration found in this study. Adjusting glycerol concentration is necessary to stabilize the dispersion of an increased quantity of graphene, as shown by the CsGlyG 06 sample film.

Acknowledgement

This work was supported by the Mechanical and Industrial Engineering Department, Universitas Gadjah Mada, and the Indonesia Endowment Fund for Education (LPDP) through the BUDI-DN program [grant number 20161141010151].

References

[1] R. C. F. Cheung, T. B. Ng, J. H. Wong, and W. Y. Chan, "Chitosan: An update on potential biomedical and pharmaceutical applications," *Mar. Drugs*, vol. 13, no. 8, pp. 5156–5186, 2015.

[2] A. Abraham, P. A. Soloman, and V. O. Rejini, "Preparation of Chitosan-Polyvinyl Alcohol Blends and Studies on Thermal and Mechanical Properties," in *Procedia Technology*, 2016, vol. 24, pp. 741–748.

[3] A. P. Martínez-camacho, M. O. Cortez-rocha, J. M. Ezquerra-brauer, and A. Z. Graciano-verdugo, "Chitosan composite films : Thermal , structural , mechanical and antifungal properties," *Carbohydr. Polym.*, vol. 82, pp. 305–315, 2010.

[4] Y. Cao, J. Feng, and P. Wu, "Preparation of organically dispersible graphene nanosheet powders through a lyophilization method and their poly (lactic acid) composites," *Carbon N. Y.*, vol. 48, no. 13, pp. 3834–3839, 2010.

[5] R. T. De Silva, M. M. M. G. P. G. Mantilaka, S. P. Ratnayake, G. A. J. Amaratunga, and K. M. N. De Silva,

"Nano-MgO reinforced chitosan nanocomposites for high performance packaging applications with improved mechanical , thermal and barrier properties," *Carbohydr. Polym.*, vol. 157, pp. 739–747, 2017.

[6] P. M. Rahman, V. M. A. Mujeeb, K. Muraleedharan, and S. K. Thomas, "Chitosan / nano ZnO composite films : Enhanced mechanical , antimicrobial and dielectric properties," *Arab. J. Chem.*, vol. 11, no. 1, pp. 120–127, 2018.

[7] J. H. R. Llanos and C. C. Tadini, "Preparation and characterization of bio-nanocomposite films based on cassava starch or chitosan , reinforced with montmorillonite or bamboo nanofibers," *Int. J. Biol. Macromol.*, vol. 107, pp. 371–382, 2018.

[8] M. Peesan, P. Supaphol, and R. Rujiravanit, "Preparation and characterization of hexanoyl chitosan / polylactide blend films," vol. 60, pp. 343–350, 2005.

[9] M. Salehi, M. Naseri Nosar, A. Amani, M. Azami, S. Tavakol, and H. Ghanbari, "Preparation of pure PLLA, pure chitosan, and PLLA/chitosan blend porous tissue engineering scaffolds by thermally induced phase separation method and evaluation of the corresponding mechanical and biological properties," *Int. J. Polym. Mater. Polym. Biomater.*, vol. 64, no. 13, pp. 675–682, 2015.

[10] N. E. Suyatma, A. Copinet, L. Tighzert, and V. Coma, "Mechanical and Barrier Properties of Biodegradable Films Made from Chitosan and Poly (Lactic Acid) Blends," vol. 12, no. 1, pp. 2–3, 2004.

[11] Z. Shariatinia and M. Fazli, "Food Hydrocolloids Mechanical properties and antibacterial activities of novel nanobiocomposite fi lms of chitosan and starch," *Food Hydrocoll.*, vol. 46, pp. 112–124, 2015.

[12] L. Ren, X. Yan, J. Zhou, J. Tong, and X. Su, "Influence of chitosan concentration on mechanical and barrier properties of corn starch / chitosan films," *Int. J. Biol. Macromol.*, vol. 105, pp. 1636–1643, 2017.

[13] L. Van Der Schueren, I. Steyaert, B. De Schoenmaker, and K. De Clerck, "Polycaprolactone/chitosan blend nanofibres electrospun from an acetic acid/formic acid solvent system," *Carbohydr. Polym.*, vol. 88, no. 4, pp. 1221–1226, 2012.

[14] A. Lauto *et al.*, "Self-expandable chitosan stent: Design and preparation," *Biomaterials*, vol. 22, no. 13, pp. 1869–1874, 2001.

[15] M.-C. Chen *et al.*, "Rapidly Self-Expandable Polymeric Stents with a Shape-Memory Property," pp. 2774–2780, 2007.

[16] M. Chen, C. Liu, H. Tsai, W. Lai, Y. Chang, and H. Sung, "Mechanical properties , drug eluting characteristics and in vivo performance of a genipin-crosslinked chitosan polymeric stent," *Biomaterials*, vol. 30, no. 29, pp. 5560–5571, 2009.

[17] B. Thierry, Y. Merhi, J. Silver, and M. Tabrizian, "Biodegradable membrane-covered stent from chitosan-based polymers," *J. Biomed. Mater. Res. Part A*, vol. 75A, no. 3, pp. 556–566, 2005.

[18] A. Ashori and R. Bahrami, "Modification of Physico-Mechanical Properties of Chitosan-Tapioca Starch Blend Films Using Nano Graphene," *Polym. Plast. Technol. Eng.*, vol. 53, pp. 312–318, 2014.

[19] D. Han, L. Yan, W. Chen, and W. Li, "Preparation of chitosan/graphene oxide composite film with enhanced mechanical strength in the wet state," *Carbohydr. Polym.*, vol. 83, no. 2, pp. 653–658, 2011.

[20] M. Fang, J. Long, W. Zhao, L. Wang, and G. Chen, "pH-Responsive Chitosan-Mediated Graphene Dispersions," *Langmuir*, vol. 26, no. 22, pp. 16771–16774, 2010.

[21] M. Cobos, B. González, M. J. Fernández, and M. D. Fernández, "Chitosan–graphene oxide nanocomposites: Effect of graphene oxide nanosheets and glycerol plasticizer on thermal and mechanical properties," *J. Appl. Polym. Sci.*, vol. 134, no. 30, pp. 1–14, 2017.

[22] H. Fan *et al.*, "Fabrication , Mechanical Properties , and Biocompatibility of Graphene-Reinforced Chitosan Composites," pp. 2345–2351, 2010.

[23] J. Li, N. Ren, J. Qiu, X. Mou, and H. Liu, "Graphene oxide-reinforced biodegradable genipin-cross-linked chitosan fluorescent biocomposite film and its cytocompatibility," *Int. J. Nanomedicine*, vol. 8, pp. 3415–3426, 2013.

[24] N. Patelis, D. Moris, S. Matheiken, and C. Klonaris, "The potential role of graphene in developing the next generation of endomaterials The potential role of graphene in developing the next generation of endomaterials," *Biomed Res. Int.*, vol. 2016, pp. 1–7, 2016.

[25] F. Jiang, Y. Yu, Y. Wang, A. Feng, and L. Song, "A novel synthesis route of graphene via microwave assisted intercalation-exfoliation of graphite," *Mater. Lett.*, vol. 200, pp. 39–42, 2017.

[26] M. Yi and Z. Shen, "Kitchen blender for producing high-quality few-layer graphene," *Carbon N. Y.*, vol. 78, pp. 622–626, 2014.

[27] G. Wang *et al.*, "Facile Synthesis and Characterization of Graphene Nanosheets," *J. Phys. Chem. C*, vol. 112, pp. 8192–8195, 2008.

[28] A. C. Tas, "The use of physiological solutions or media in calcium phosphate synthesis and processing," *Acta Biomater.*, vol. 10, pp. 1771–1792, 2014.

[29] T. Kokubo, "Surface Chemistry of Bioactive Glass-Ceramics," *J. Non. Cryst. Solids*, vol. 120, pp. 138–151, 1990.

[30] M. Naebe *et al.*, "Mechanical Property and Structure of Covalent Functionalised Graphene/Epoxy

Nanocomposites," *Sci. Rep.*, vol. 4, pp. 1–7, 2014.
[31] M. W. Lee, T. Y. Wang, and J. L. Tsai, "Mechanical properties of nanocomposites with functionalized graphene," *J. Compos. Mater.*, vol. 50, no. 27, pp. 3779–3789, 2016.
[32] T. Kuilla, S. Bhadra, D. Yao, N. H. Kim, S. Bose, and J. H. Lee, "Recent advances in graphene based polymer composites," *Prog. Polym. Sci.*, vol. 35, no. 11, pp. 1350–1375, 2010.
[33] X. Yang, Y. Tu, L. Li, S. Shang, and X. Tao, "Well-Dispersed Chitosan/Graphene Oxide Nanocomposites," *Appl. Mater. Interfaces*, vol. 2, no. 6, pp. 1707–1713, 2010.
[34] K. W. Putz, O. C. Compton, M. J. Palmeri, S. B. T. Nguyen, and L. C. Brinson, "High-nanofiller-content graphene oxide-polymer nanocomposites via vacuum-assisted self-assembly," *Adv. Funct. Mater.*, vol. 20, no. 19, pp. 3322–3329, 2010.
[35] F. Croisier and C. Jérôme, "Chitosan-based biomaterials for tissue engineering," *Eur. Polym. J.*, vol. 49, no. 4, pp. 780–792, 2013.
[36] H. Zhuang, J. P. Zheng, H. Gao, and K. De Yao, "In vitro biodegradation and biocompatibility of gelatin / montmorillonite-chitosan intercalated nanocomposite," *J. Mater. Sci. Mater. Med.*, vol. 18, pp. 951–957, 2007.